



CHORUS

This is the accepted manuscript made available via CHORUS. The article has been published as:

Spatial Markov Model of Anomalous Transport Through Random Lattice Networks

Peter K. Kang, Marco Dentz, Tanguy Le Borgne, and Ruben Juanes

Phys. Rev. Lett. **107**, 180602 — Published 27 October 2011

DOI: [10.1103/PhysRevLett.107.180602](https://doi.org/10.1103/PhysRevLett.107.180602)

Spatial Markov Model of Anomalous Transport Through Random Lattice Networks

Peter K. Kang,¹ Marco Dentz,² Tanguy Le Borgne,³ and Ruben Juanes¹

¹*Massachusetts Institute of Technology, 77 Massachusetts Ave, Building 48, Cambridge, Massachusetts 02139, USA*

²*Spanish National Research Council (IDAEA-CSIC), c/ Jordi Girona 18-26, 08034 Barcelona, Spain*

³*Université de Rennes 1, CNRS, Geosciences Rennes, UMR 6118, Rennes, France*

(Dated: September 29, 2011)

Flow through lattice networks with quenched disorder exhibits strong correlation in the velocity field, even if the link transmissivities are uncorrelated. This feature, which is a consequence of the divergence-free constraint, induces anomalous transport of passive particles carried by the flow. We propose a Lagrangian statistical model that takes the form of a continuous time random walk (CTRW) with correlated velocities derived from a genuinely multidimensional Markov process in space. The model captures the anomalous (non-Fickian) longitudinal and transverse spreading, and the tail of the mean first passage time observed in the Monte Carlo simulations of particle transport. We show that reproducing these fundamental aspects of transport in disordered systems requires honoring the correlation in the Lagrangian velocity.

PACS numbers: 05.60.Cd, 05.40.Fb, 05.10.Gg, 92.40.Kf

Anomalous transport, understood as the nonlinear scaling with time of the mean square displacement of transported particles, is observed in many physical processes, including contaminant transport through porous and fractured geologic media [1], animal foraging patterns [2], freely diffusing molecules in tissue [3], tracer diffusion in suspensions of swimming micro-organisms [4], and biased transport in complex networks [5].

Anomalous transport often leads to a broad-ranged particle distribution density, both in space and time [6–8]. Understanding the origin of the slow-decaying tails in probability density is essential, because they determine the likelihood of high-impact, “low-probability” events and therefore exert a dominant control over the predictability of a system [9]. This becomes especially important when human health is at risk, such as in epidemic spreading through transportation systems [10] or radionuclide transport in the subsurface [11].

Past studies have shown that high variability in the flow properties leads to anomalous transport [1, 7]. Depending on the nature of the underlying disorder distribution anomalous behavior can be transient or persist to asymptotic scales [12, 13]. The continuous time random walk (CTRW) formalism [14, 15] offers an attractive framework to understand and model anomalous transport through disordered media and networks [1, 5, 16]. The CTRW model is intrinsically an annealed model because the disorder configuration changes at each random-walk step. A particle that returns to the same position experiences different velocity properties. The validity of the CTRW approach for average transport in quenched random environments has been studied for purely diffusive transport [e.g., 7] and biased diffusion [e.g., 9, 17–19]. Most studies that employ the CTRW approach assume that transition times associated with particle displacements are independent of each other, therefore neglecting velocity correlation between successive jumps [20]. Indeed, a recent study of transport on a lattice network has shown that CTRW with independent transition times emerges as an exact macroscopic transport model when velocities are uncorrelated [9].

However, detailed analysis of particle transport simulations demonstrates conclusively that particle velocities in mass-conservative flow fields exhibit correlation along their spatial trajectory [17, 21, 22]. Mass conservation induces correlation in the Eulerian velocity field because fluxes must satisfy the divergence-free constraint at each intersection. This, in turn, induces correlation in the velocity sequence along a particle trajectory. To take into account velocity correlation, Lagrangian models based on temporal [22, 23] and spatial [17, 21] Markovian processes have recently been proposed. These models successfully capture many important aspects of the Lagrangian velocity statistics and the particle transport behavior. In particular, the study of Le Borgne et al. [17] shows that introducing correlation in the Lagrangian velocity through a Markov process in space yields an accurate representation of the first and second moments of the particle density. The model is restricted, however, to particle trajectories projected onto the direction of the mean flow, and the study leaves open the question of whether spatial Markov processes can describe multidimensional features of transport.

Here, we investigate average transport in divergence-free flow through a quenched random lattice from the CTRW point of view. We introduce a multidimensional spatial Markov model for particle velocity, and confirm that the model exhibits excellent agreement with Monte Carlo simulations. We show that accounting for the spatial correlation in the Lagrangian velocity is essential to capture the fundamental macroscopic transport behavior.

Random Lattice Network. We consider a lattice network consisting of two sets of parallel, equidistant links oriented at an angle of $\pm\alpha$ with the x -axis. The distance between nodes is l [Fig. 1(a)]. Flow through the network is modeled by assuming Darcy’s law [24] for the fluid flux u_{ij} between nodes i and j , $u_{ij} = -k_{ij}(\Phi_j - \Phi_i)/l$, where Φ_i and Φ_j are the flow potentials, and $k_{ij} > 0$ is the conductivity of the link between the two nodes. Imposing mass conservation at each node i , $\sum_j u_{ij} = 0$, leads to a linear system of equations, which is solved for the flow potentials at the nodes. A link from node i to j is incoming for $u_{ij} < 0$ and outgoing for $u_{ij} > 0$. We denote by \mathbf{e}_{ij} the unit vector in the direction of the link connecting i and j . A realization of the random lattice network is generated by assigning independent and identically distributed random conductivities to each link. Therefore, the k values in different links are uncorrelated. The set of all realizations of the quenched random network generated in this way form a statistical ensemble that is stationary and ergodic.

We study a simple flow setting of mean flow in the positive x -direction, by imposing a no-flow condition at the top and bottom boundaries of the network, and fixed values of the potential at the left ($\Phi = 1$) and right ($\Phi = 0$) boundaries.

Once the fluxes at the links are known, we simulate transport of a passive tracer by particle tracking. We neglect diffusion along links, and thus particles are advected with the flow velocity between nodes. We assume complete mixing at the nodes. Thus, the link through which the particle exits a node is chosen randomly with flux-weighted probability. The Langevin equations describing particle movements in space and time are

$$\mathbf{x}_{n+1} = \mathbf{x}_n + l \frac{\mathbf{v}(\mathbf{x}_n)}{|\mathbf{v}(\mathbf{x}_n)|}, \quad t_{n+1} = t_n + \frac{l}{|\mathbf{v}(\mathbf{x}_n)|}. \quad (1)$$

If \mathbf{x}_n is the position of the i th node, the transition velocity is equal to $\mathbf{v}(\mathbf{x}_n) = u_{ij}\mathbf{e}_{ij}$ with probability $p_{ij} = |u_{ij}|/\sum_k |u_{ik}|$ where the summation is over outgoing links only, and $p_{ij} = 0$ for incoming links. The velocity vector \mathbf{v} in the following is expressed in (ν, θ) coordinates, in which $\nu = |v| \cos(\varphi)/|\cos(\varphi)|$ is the velocity along a link with $\varphi = \arccos(v_x/|v|)$ and $\theta = \sin(\varphi)/|\sin(\varphi)|$, so that $\mathbf{v} = [\nu \cos(\alpha), |\nu|\theta \sin(\alpha)]^t$. Note that φ can only assume values in $\{-\alpha, \alpha, \pi - \alpha, \pi + \alpha\}$.

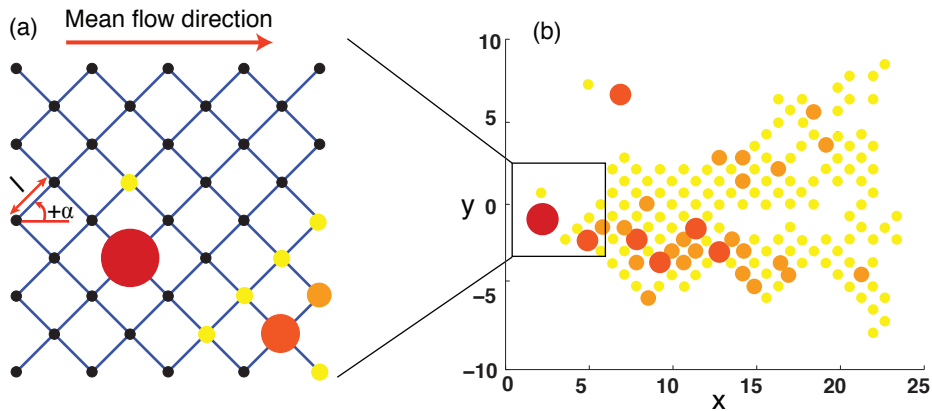


FIG. 1. (a) Schematic of the lattice network considered here, with two sets of links with orientation $\pm\alpha = \pm\pi/4$ and spacing $l = 1$. (b) Particle distribution at nodes (represented by circles of different sizes) at $t = 30$ for a single realization after injection at the origin at $t = 0$.

The system of discrete Langevin equations (1) describes coarse-grained particle transport for a single realization of the quenched random lattice. Particle velocities and thus transition times depend on the particle position. The particle position at time t is $\mathbf{x}(t) = \mathbf{x}_{n_t}$, where n_t denotes the number of steps needed to reach time t . The mean particle density is $P(\mathbf{x}, t) = \langle \delta(\mathbf{x} - \mathbf{x}_{n_t}) \rangle$, where the angular brackets denote both the noise average over all particles in one realization and the ensemble average over all network realizations. We solve transport in a single disorder realization by particle tracking based on Eq. (1) with the initial conditions $\mathbf{x}_0 = \mathbf{0}$ and $t_0 = 0$ [Fig. 1(b)]. From this, we obtain the mean particle density $P(\mathbf{x}, t)$ by ensemble averaging.

To develop a transport model for the average particle density $P(\mathbf{x}, t)$, we study average particle movements from a CTRW point of view. This could be done, for example, by interpreting first-passage time distributions in the CTRW framework and inferring an optimal distribution of transition times [20]. Here we follow a different rationale and analyze the ensemble statistics of the Lagrangian velocities because the CTRW model is based on the assumption that particle velocities sampled at given spatial positions along an average trajectory form a Markov process.

Spatial Markov Property. To characterize average particle movement from a CTRW point of view, we study the ensemble statistics of the series of Lagrangian velocities experienced by particles along individual trajectories. We consider the transition probability density to encounter a velocity \mathbf{v} after $n + m$ steps given that the particle velocity was \mathbf{v}' after n steps, which in the variables (ν, θ) reads

$$r_m(\nu, \theta | \nu', \theta') = \langle \delta[\nu - \nu(\mathbf{x}_{n+m})] \delta_{\theta, \theta(\mathbf{x}_{n+m})} \rangle \Big|_{\nu(\mathbf{x}_n) = \nu', \theta(\mathbf{x}_n) = \theta'}. \quad (2)$$

We study the statistical properties of the Lagrangian velocity $\mathbf{v}(\mathbf{x}_n)$ by particle tracking simulations in 10^3 realizations of an ensemble of random lattices characterized by a lognormal k distribution with variance $\sigma_{\ln k}^2 = 5$. The use of a lognormal distribution is motivated by measurements of conductivity in many natural media [25]. The lattice size is 500×500 nodes and, in each realization, we release 10^3 particles at the origin. To evaluate the transition probability numerically, the particle velocity ν is discretized into classes, $\nu \in \bigcup_{j=1}^N (\nu_j, \nu_{j+1})$. To emphasize the role of low velocities, velocity classes are defined on a near-logarithmic scale. We define the transition probability matrix

$$T_m(i, \theta | j, \theta') = \int_{\nu_i}^{\nu_{i+1}} d\nu \int_{\nu_j}^{\nu_{j+1}} d\nu' r_m(\nu, \theta | \nu', \theta'). \quad (3)$$

The aggregate transition matrix $T_m(i|j) = \sum_{\theta, \theta'} T_m(i, \theta | j, \theta')$ shown in Fig. 2a for $m = 1$, clearly indicates that particle velocities are correlated. The relatively large probabilities in the upper-left and lower-right corners of the transition matrix reflect flow reversal.

The series of Lagrangian velocities $\mathbf{v}(\mathbf{x}_n) \equiv \mathbf{v}_n$ along particle trajectories can be approximated as a Markov process, if the transition matrix satisfies the Chapman-Kolmogorov equation [e.g., 26], which in matrix form reads

$$T_n(i, \theta | j, \theta') = \sum_{i', \theta''} T_{n-m}(i, \theta | i', \theta'') T_m(i', \theta'' | j, \theta'). \quad (4)$$

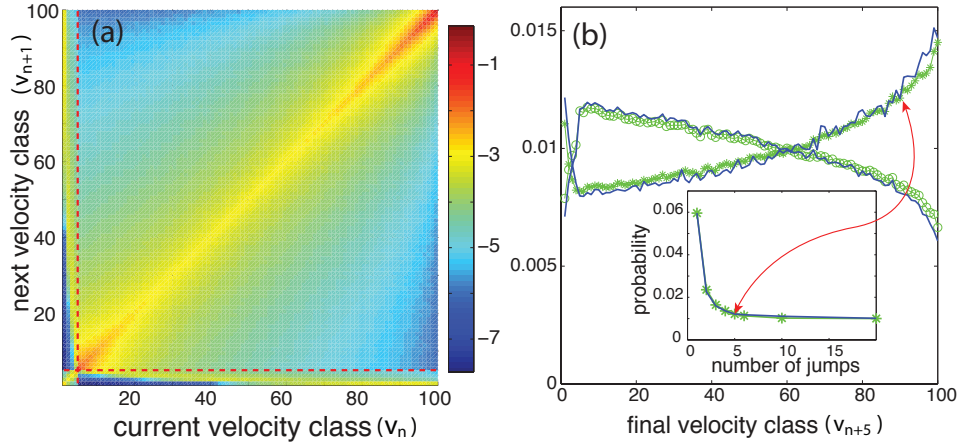


FIG. 2. (a) Aggregate transition matrix for $N = 100$ velocity classes distributed with logarithmic scale. (b) Transition probabilities after $m = 5$ steps from direct Monte Carlo computation (blue solid line) and calculated from the Markov assumption (green symbols). Shown are probability densities for two initial velocity classes: a low velocity class ($j = 5$, \circ), and a high velocity class ($j = 90$, $*$). Inset: probability of returning to the same initial velocity class as a function of the number of steps for a high initial velocity (class $j = 90$).

Specifically, for a Markov process, the m -step transition matrix \mathbf{T}_m is equal to the m -fold product of the 1-step transition matrix \mathbf{T}_1 with itself as $\mathbf{T}_m = \mathbf{T}_1^m$. Figure 2c shows the transition probabilities for $m = 5$ steps conditional to a low ($j = 5$) and high ($j = 90$) velocity class given by \mathbf{T}_5 , which is obtained by direct Monte Carlo simulations, and under the Markov assumption from \mathbf{T}_1^5 . The Markov model predicts accurately the transition probabilities, as well as the return probability for any number of steps [Fig. 2b, inset]. Our analysis suggests that the Markov model captures the Lagrangian velocity statistics accurately. We repeated the analysis for truncated power-law and the absolute value of Cauchy distributions of conductivity, and found that the Markovianity assumption holds for these conductivity distributions too. Therefore, a CTRW characterized by a one step correlation in velocity is a good approximation for describing average transport.

Continuous Time Random Walk Model. Particle movements in the random lattice can, on average, be described by the following system of Langevin equations

$$\mathbf{x}_{n+1} = \mathbf{x}_n + l \frac{\mathbf{v}_n}{|\mathbf{v}_n|}, \quad t_{n+1} = t_n + \frac{l}{|\mathbf{v}_n|}. \quad (5)$$

We have already shown that the series of Lagrangian velocities $\{\mathbf{v}_n\}_{n=0}^{\infty}$ is well approximated by a Markov process and thus fully characterized by the one-point density $p(\mathbf{v}) = \langle \delta(\mathbf{v} - \mathbf{v}_n) \rangle$ and the one-step transition probability density

$$r_1(\mathbf{v}|\mathbf{v}') = \langle \delta(\mathbf{v} - \mathbf{v}_{n+1}) \rangle_{|\mathbf{v}_n = \mathbf{v}'}. \quad (6)$$

The particle density can be written as

$$P(\mathbf{x}, t) = \int d\mathbf{v} \langle \delta(\mathbf{x} - \mathbf{x}_{n_t}) \delta(\mathbf{v} - \mathbf{v}_{n_t}) \rangle, \quad (7)$$

in which $n_t = \max(n | t_n \leq t)$, \mathbf{x} is the position of the node at which the particle is at time t , and \mathbf{v} is the velocity by which the particle emanates from this node. Equation (7) can be recast as

$$P(\mathbf{x}, t) = \int d\mathbf{v} \int_{t-l/|\mathbf{v}|}^t dt' R(\mathbf{x}, \mathbf{v}, t'), \quad (8a)$$

in which we defined

$$R(\mathbf{x}, \mathbf{v}, t') = \sum_{n=0}^{\infty} \langle \delta(\mathbf{x} - \mathbf{x}_n) \delta(\mathbf{v} - \mathbf{v}_n) \delta(t' - t_n) \rangle. \quad (8b)$$

The latter satisfies the Kolmogorov type equation

$$R(\mathbf{x}, \mathbf{v}, t) = \delta(\mathbf{x})p(\mathbf{v})\delta(t) + \int d\mathbf{v}' r_1(\mathbf{v}|\mathbf{v}') \\ \times \int d\mathbf{x}' \delta(\mathbf{x} - \mathbf{x}' - l\mathbf{v}'/|\mathbf{v}'|)R(\mathbf{x}', \mathbf{v}', t - l/|\mathbf{v}'|). \quad (8c)$$

For independent successive velocities, i.e., $r_1(\mathbf{v}|\mathbf{v}') = p(\mathbf{v})$, one recovers the CTRW model [e.g., 14]

$$P(\mathbf{x}, t) = \int_0^t dt' R(\mathbf{x}, t') \int_{t-t'}^\infty d\tau \int d\mathbf{x}' \psi(\mathbf{x}, \tau), \quad (9a)$$

where $R(\mathbf{x}, t)$ satisfies

$$R(\mathbf{x}, t) = \delta(\mathbf{x})\delta(t) \\ + \int d\mathbf{x}' \int_0^t dt' R(\mathbf{x}', t') \psi(\mathbf{x} - \mathbf{x}', t - t') \quad (9b)$$

and the joint transition length and time density is given by

$$\psi(\mathbf{x}, t) = \int d\mathbf{v}' p(\mathbf{v}') \delta(\mathbf{x} - l\mathbf{v}'/|\mathbf{v}'|) \delta(t - l/|\mathbf{v}'|). \quad (9c)$$

In the following, we refer to system (8) as *correlated* CTRW because subsequent particle velocities are correlated, and to model (9) as *uncorrelated* CTRW because subsequent particle velocities are uncorrelated.

Average Transport Behavior. The average transport behavior is studied in terms of the spatial particle density $P(\mathbf{x}, t)$, its mean square displacements in longitudinal and transverse directions and the distribution of the first passage time, $t_f(x)$, at a control plane at a distance x from the inlet. We compare the results obtained from direct Monte Carlo simulations to correlated CTRW and uncorrelated CTRW. Correlated CTRW is parametrized by the one-step transition matrix \mathbf{T}_1 determined from numerical Monte Carlo simulations. Uncorrelated CTRW is parametrized by the Lagrangian velocity distribution $p(\mathbf{v})$, which is obtained from Monte Carlo simulations as well.

The particle distribution is non-Gaussian and characterized by a sharp leading edge and an elongated tail [Fig. 3]. The non-Gaussian features persist even after the center of mass has travelled a distance of about 100 links in the direction of the mean flow. Correlated CTRW captures the shape of the particle plume with remarkable accuracy, including its leading edge, peak, transverse spread, and low-probability tail near the origin. Ignoring the correlated structure of the Lagrangian velocity leads to predictions of longitudinal and transverse spreading that deviate from the direct Monte Carlo simulation [Fig. 3, insets].

Figure 4a shows the time evolution of the longitudinal and transverse spreading. The Monte Carlo simulation shows that the longitudinal mean square displacement (MSD) with respect to the center of mass evolves faster than linear with time (slope of 1.33). Both the scaling and the magnitude of the longitudinal spreading are captured accurately by correlated CTRW. The model also reproduces accurately the magnitude and time scaling of the transverse MSD. The uncorrelated model underpredicts the magnitude of longitudinal spreading.

Nonlocal theories of transport, including CTRW, are often invoked to explain the empirical observation that the first passage time (FPT) distribution is broad-ranged [1]. Early arrival and slow decay of the FPT is also observed in our model system, even when the conductivity distribution is lognormal and has zero spatial correlation [Fig. 4(b)]. The cumulative FPT distribution from the Monte Carlo simulation exhibits a significantly slower decay than uncorrelated CTRW. This behavior is accurately captured by correlated CTRW, suggesting that the velocity correlation along particle trajectories is responsible for the emergence of the observed asymptotic behavior.

In conclusion, we have shown that the divergence-free condition arising from mass conservation is the source of strong and nontrivial correlation in the Lagrangian velocity, even when the underlying conductivity field is completely uncorrelated. Accounting for such correlation in the velocity is important to obtain quantitative agreement for the mean particle density and the FPT distribution. Here, we have proposed and validated a spatial Markov model of transport on a lattice network that explicitly captures the multidimensional effects associated with changes in direction along the particle trajectory. This study opens the door to understanding the interplay between two sources of velocity correlation: the divergence-free condition and the spatial correlation in the permeability field. Finally, we suspect that correlation in the Lagrangian velocity exerts an even more dominant control over mixing (understood as the decay of the variance of the particle density [27–29]) than it does on spreading. This remains an exciting open question.

We gratefully acknowledge funding for this research, provided by the DOE Office of Science Graduate Fellowship Program (to PKK), the Spanish Ministry of Science and Innovation through the project HEART (CGL2010-18450) (to MD), the European

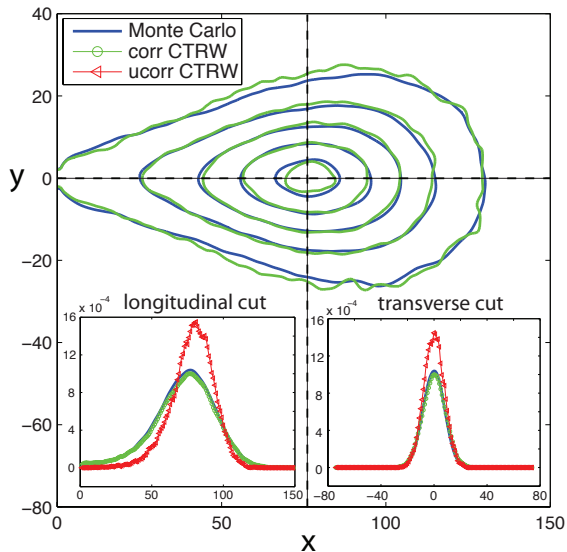


FIG. 3. Contour plot of the mean particle density at $t = 5 \times 10^2$, computed from direct Monte Carlo simulation (blue solid line), correlated CTRW model (green solid line), and uncorrelated CTRW model (red solid line).

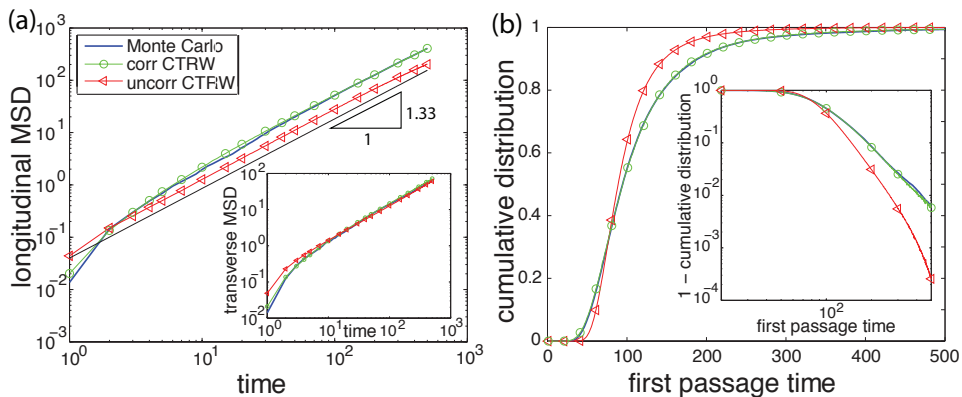


FIG. 4. (a) Time evolution of the longitudinal MSD. Inset: Transverse MSD. (b) Cumulative FPT distribution.

commission through the ITN network IMVUL (Grant Agreement 212298) and ERG grant ReactiveFlows (Grant Agreement 230947) (to TLB), and Eni S.p.A. under the Multiscale Reservoir Science project and the ARCO Chair in Energy Studies (to RJ).

-
- [1] B. Berkowitz, A. Cortis, M. Dentz, and H. Scher, *Rev. Geophys.* **44**, RG2003 (2006).
- [2] G. M. Viswanathan, V. Afanasyev, S. V. Buldyrev, E. J. Murphy, P. A. Prince, and H. E. Stanley, *Nature* **381**, 413 (1996).
- [3] S. R. Yu, M. Burkhardt, M. N. ad J. Ries, Z. Petrášek, S. Scholpp, P. Schwille, and M. Brand, *Nature* **461**, 533 (2009).
- [4] K. C. Leptos, J. S. Guasto, J. P. Gollub, A. I. Pesci, and R. E. Goldstein, *Phys. Rev. Lett.* **103**, 198103 (2009).
- [5] C. Nicolaides, L. Cueto-Felgueroso, and R. Juanes, *Phys. Rev. E* **82**, 055101(R) (2010).
- [6] M. F. Shlesinger, *J. Stat. Phys.* **10**, 421 (1974).
- [7] J. P. Bouchaud and A. Georges, *Phys. Rep.* **195**, 127 (1990).
- [8] R. Metzler and J. Klafter, *Phys. Rep.* **339**, 1 (2000).
- [9] P. K. Kang, M. Dentz, and R. Juanes, *Phys. Rev. E* **83**, 030101(R) (2011).
- [10] D. Balcan, V. Colizza, B. Gonçalves, H. Hu, J. J. Ramasco, and A. Vespignani, *Proc. Natl. Acad. Sci. USA* **106**, 21484 (2009).
- [11] J. Molinero and J. Samper, *J. Contaminant Hydrol.* **82**, 293 (2006).
- [12] M. G. Trefry, F. P. Ruan, and D. McLaughlin, *Water Resour. Res.* **39**, 1063 (2003).
- [13] M. Dentz, A. Cortis, H. Scher, and B. Berkowitz, *Adv. Water Resour.* **27**, 155 (2004).
- [14] H. Scher and E. W. Montroll, *Phys. Rev. B* **12**, 2455 (1975).
- [15] J. Klafter and R. Silbey, *Phys. Rev. Lett.* **44**, 55 (1980).
- [16] B. Berkowitz and H. Scher, *Phys. Rev. Lett.* **79**, 4038 (1997).
- [17] T. Le Borgne, M. Dentz, and J. Carrera, *Phys. Rev. Lett.* **101**, 090601 (2008).
- [18] M. Dentz and A. Castro, *Geophys. Res. Lett.* **36**, L03403 (2009).
- [19] M. Dentz and D. Bolster, *Phys. Rev. Lett.* **105**, 244301 (2010).
- [20] B. Berkowitz and H. Scher, *Phys. Rev. E* **81**, 011128 (2010).
- [21] R. Benke and S. Painter, *Water Resour. Res.* **39**, 1324 (2003).
- [22] D. W. Meyer and H. A. Tchelepi, *Water Resour. Res.* **46**, W11552 (2010).
- [23] S. Painter and V. Cvetkovic, *Water Resour. Res.* **41**, W02002 (2005).
- [24] J. Bear, *Dynamics of Fluids in Porous Media* (Elsevier, 1972).
- [25] X. Sanchez-Vila, A. Guadagnini, and J. Carrera, *Rev. Geophys.* **44**, RG3002 (2006).
- [26] H. Risken, *The Fokker-Planck Equation*, 2nd ed. (Springer, Berlin, 1989).
- [27] T. Le Borgne, M. Dentz, D. Bolster, J. Carrera, J.-R. de Dreuzy, and P. Davy, *Adv. Water Resour.* **33**, 1468 (2010).
- [28] B. Jha, L. Cueto-Felgueroso, and R. Juanes, *Phys. Rev. Lett.* **106**, 194502 (2011).
- [29] A. M. Tartakovsky, D. M. Tartakovsky, and P. Meakin, *Phys. Rev. Lett.* **101**, 044502 (2008).